Pergamon

Int. J. Heat Mass Transfer. Vol. 39, No. 10, pp. 2067–2075, 1996

0017-9310/96 $15.00 + 0.00

0017-9310(95)00299-5

Interfacial wave stability of concurrent two-phase flow in a horizontal channel

Q. WU and M. ISHII

Laboratory of Thermal-Hydraulics and Reactor Safety, School of Nuclear Engineering, Purdue University, West Lafayette, IN 47907, U.S.A.

(*Received* 22 *February* 1995 *and in final form* 27 *July* 1995)

Abstract—A wave front perturbation method is applied to a one-dimensional two-phase flow in a horizontal duct to analyze the interfacial wave stability. The governing equations are thus reduced to a first-order ordinary differential equation (ODE). The linear solution of this ODE agrees with the conclusion from the small amplitude wave perturbation approach. The non-linear theory suggests that the linear stability result is sufficient for predicting instability in wavy flow, and may over-predict the critical gas velocity for large disturbances. Accordingly, a weak non-linear stability criterion is obtained. The type of unstable wave, under-cut wave or roll wave, also can be predicted analytically. Copyright © 1996 Elsevier Science Ltd.

INTRODUCTION

In a horizontal duct, the onset of interfacial wave instability for a separated gas–liquid wavy flow is usually related to the wavy-slug flow regime transition. The conventional approach to analyze this wave stability problem is to linearize the governing equations and to seek traveling wave solutions, resulting in a quadratic algebraic characteristic equation that involves the wave propagating velocity C. If the solution of this velocity has an imaginary part, waves are unstable. It implies that disturbances of any sizes will be amplified exponentially with respect to time. Following this approach, the classical inviscid Kelvin–Helmholtz stability criterion is obtained in the following form to predict the critical relative velocity between the gas phase and the liquid phase in a horizontal duct:

$$(V_g - V_f) \geqslant \sqrt{\frac{(\rho_f - \rho_g) g h_g}{\rho_g}}, \qquad (1)$$

where V_g, ρ_g, V_f, ρ_f, h_g, and g stand for gas velocity, gas density, liquid velocity, liquid density, gas chamber height (Fig. 1), and the gravitational acceleration, respectively. When the relative velocity is larger than a certain critical value, the suction effect resulting from the gas pressure variation over a wave bump overcomes the stabilizing effects. Accordingly, waves begin to grow, resulting in slug formation. However, experimental data [2–4] show that the critical relative gas velocity is much smaller than the value predicted by above criterion. In 1976, Taitel and Dukler [5] developed a correlation based on the major force balance on an inviscid interfacial wave of finite amplitude, and proposed a factor K to modify the K–H instability. This factor was gas void fraction dependent, and agreed with the experimental results of Mandhane. A theoretical approach was introduced earlier by Kordyban and Ranov [6] to consider inviscid waves of finite amplitude. They suggested that the effect of K–H instability could be enhanced in a closed duct because of the non-linear terms in the governing equations. They derived a modifying factor K as a function of wave number k, as well as gas void fraction. It required the knowledge of the wave number k at the point of slug formation. To avoid this inconvenience, Mishima and Ishii [7] applied the concept of 'most dangerous wave' to Kordyban's method and achieved an analytical solution of the modification factor K equal to 0.487, which was close to 0.5, the experimental results of Wallis and Dobson [2].

Some investigators [8–10] suggested that friction effects played an important role in slug formation. They solved the linearized field equations with interfacial and wall friction effects by means of a small amplitude perturbation technique. Their results were consistent with the existing experimental data for two-phase pipe flow. The underlying mechanism of this approach, as pointed out by Wallis in 1969 [1], was that instability occurred whenever the continuity wave overtook the dynamic wave. Recently, Barnea and Taitel [11] analyzed the existence of multiple steady-state solutions for stratified flow, and proposed a con-

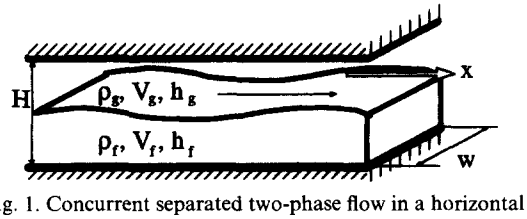

Fig. 1. Concurrent separated two-phase flow in a horizontal duct.

NOMENCLATURE

A	coefficient matrix
b	term defined in the text
C	wave velocity
F	friction term
f	friction factor
G	$(\rho_f-\rho_g)Hg/\rho_g$
g	gravitational acceleration
H	channel height
h	fluid height
j	superficial velocity
K	constant
k	wave number
P	pressure
R	channel aspect ratio
t	time
V	velocity
v	relative velocity
W	channel width
x	horizontal coordinate.

Greek symbols

α	gas void fraction (h_g/H)
φ	term defined in the text
γ	ratios defined in the text
η	wave height
ρ	fluid density
σ	terms defined in the text
τ	time constant (σ_1/σ_3)
ξ	wave front coordinate $(Ct-x)$
ζ	term defined in the text.

Subscripts

0	undisturbed state
1	first-order variable or index for σ
2	second-order variable or index for σ
3	index for σ
+	forward wave
−	backward wave
*	dimensionless parameter
b	wave break condition
cr	critical value
d	dynamic wave
f	liquid phase or friction factor
g	gas phase
i	interface
w	continuity wave.

cept of structural stability to identify the possible stable equilibrium conditions. They concluded that only the thinnest steady surface level could be physically observed, and thus the linear perturbation should only be applied to this steady-state. In 1994 they extended their studies to the analysis of non-linear wave stability via a numerical method [12]. Their results appeared to support the linear theory.

In the present research, a different technique, wave front perturbation, is applied to a one-dimensional, viscous, concurrent, separated two-phase flow in a horizontal rectangular duct. The original partial differential equations are subsequently reduced to a first-order non-linear ordinary differential equation containing only the first-order perturbed variable. The linear solution of this ODE agrees with the conclusion of a small amplitude wave perturbation method with friction effects [1], i.e. instability occurs if the continuity wave overtakes the dynamic wave. However, in the case of air-water concurrent flow for instance, this criterion is valid only for the forward waves. According to the new method, backward waves are unconditional stable. With weakly non-linear effects, the full solution of the ODE suggests that the linear stability result is a sufficient condition for stratified wavy flow to be unstable, and may over-predict the critical gas velocity, especially when there exist large external disturbances. Accordingly, a weakly non-linear wave instability criterion is obtained. However, information of the initial disturbance is needed to practically predict the occurrence of wave instability. Furthermore, the type of unstable waves, under-cut waves or roll waves, can be predicted analytically in terms of the non-linear effects.

WAVE FRONT PERTURBATION

For a one-dimensional, viscous, concurrent, separated two-phase flow in a horizontal rectangular duct with the liquid phase at the bottom part (Fig. 1), the governing equations for the two phases are derived [1] in the following form by assuming no phase change, no surface tension effect, incompressible fluids, and turbulent isothermal flows.

Continuity equations

$$\frac{\partial\alpha}{\partial t}+\frac{\partial\alpha V_g}{\partial x}=0 \tag{2}$$

$$\frac{\partial(1-\alpha)}{\partial t}+\frac{\partial(1-\alpha)V_f}{\partial x}=0. \tag{3}$$

Momentum equations

$$\rho_g\left(\frac{\partial V_g}{\partial t}+V_g\frac{\partial V_g}{\partial x}\right)=-\frac{\partial P}{\partial x}-\frac{f_g}{2}\rho_g V_g^2\left(\frac{1}{H\alpha}+\frac{2}{W}\right)$$
$$-\frac{f_i}{2H\alpha}\rho_g(V_g-V_f)|V_g-V_f| \tag{4}$$

$$\rho_f\left(\frac{\partial V_f}{\partial t}+V_f\frac{\partial V_f}{\partial x}\right)=-\frac{\partial P}{\partial x}-(\rho_f-\rho_g)gH\frac{\partial \alpha}{\partial x}$$
$$-\frac{f_f}{2}\rho_f V_f^2\left(\frac{1}{H(1-\alpha)}+\frac{2}{W}\right)$$
$$+\frac{f_i}{2H(1-\alpha)}\rho_g(V_g-V_f)|V_g-V_f|, \quad (5)$$

where α is the area averaged gas void fraction representing h_g/H, H and W are the channel height and width, P, ρ_g, ρ_f, V_g, V_f, f_f, f_g and f_i denote pressure, gas density, liquid density, gas velocity, liquid velocity, liquid side wall friction factor, gas side wall friction factor, and interfacial friction factor, respectively. The x coordinate is in the flow direction as shown in Fig. 1. By combining equations (4) and (5) to eliminate pressure gradient terms, we then have

$$\left(\frac{\partial V_g}{\partial t}+V_g\frac{\partial V_g}{\partial x}\right)-\gamma_{pfg}\left(\frac{\partial V_f}{\partial t}+V_f\frac{\partial V_f}{\partial x}\right)$$
$$=-G\frac{\partial \alpha}{\partial x}+F(\alpha, V_g, V_f) \quad (6)$$

$$F(\alpha, V_g, V_f)=\frac{f_f}{2}\gamma_{pfg}V_f^2\left(\frac{1}{H(1-\alpha)}+\frac{2}{W}\right)$$
$$-\frac{f_i}{2H\alpha(1-\alpha)}(V_g-V_f)|V_g-V_f|$$
$$-\frac{f_g}{2}V_g^2\left(\frac{1}{H\alpha}+\frac{2}{W}\right) \quad (7)$$

$$G=(\rho_f-\rho_g)gH/\rho_g \qquad \gamma_{pfg}=\rho_f/\rho_g.$$

Equations (2), (3) and (6) constitute a system of partial differential equations, to which the wave front perturbation technique can be applied [13]. Since the system admits a steady solution that satisfies $F(\alpha_0, V_{g0}, V_{f0})=0$, these equations can thus be perturbed around the steady state by tracing the wave front of a disturbance and expanding the variables in power of $\xi=(Ct-x)$. Here C stands for the wave front propagation velocity, and ξ equals zero at the wave front where the liquid level is neutral.

$$\alpha=\alpha_0+\alpha_1(t)\xi+\tfrac{1}{2}\alpha_2(t)\xi^2+\cdots$$
$$V_g=V_{g0}+V_{g1}(t)\xi+\tfrac{1}{2}V_{g2}(t)\xi^2+\cdots$$
$$V_f=V_{f0}+V_{f1}(t)\xi+\tfrac{1}{2}V_{f2}(t)\xi^2+\cdots$$

By substituting these expansions into equations (2), (3) and (6), and equating the successive terms in powers of ξ to zero, the following equations from the first-order and the second-order terms are obtained:

$$[A]\begin{Bmatrix}\alpha_1\\V_{g1}\\V_{f1}\end{Bmatrix}=0$$

$$[A]=\begin{bmatrix}(V_{g0}-C) & \alpha_0 & 0\\(V_{f0}-C) & 0 & -(1-\alpha_0)\\G & (V_{g0}-C) & -\gamma_{pfg}(V_{f0}-C)\end{bmatrix} \quad (8)$$

$$[A]\begin{Bmatrix}\alpha_2\\V_{g2}\\V_{f2}\end{Bmatrix}=\{B\}$$

$$\{B\}=\begin{Bmatrix}(d\alpha_1/dt-2\alpha_1V_{g1})\\(d\alpha_1/dt-2\alpha_1V_{f1})\\-F_1-\gamma_{pfg}\left(dV_{f1}/dt-V_{f1}^2\right)+\left(dV_{g1}/dt-V_{g1}^2\right)\end{Bmatrix} \quad (9)$$

$$F_1=\alpha_1\left.\frac{\partial F}{\partial \alpha}\right|_{\alpha_0,V_{g0},V_{f0}}+V_{g1}\left.\frac{\partial F}{\partial V_g}\right|_{\alpha_0,V_{g0},V_{f0}}+V_{f1}\left.\frac{\partial F}{\partial V_f}\right|_{\alpha_0,V_{g0},V_{f0}}.$$

The first-order equation [equation (8)] is homogeneous. For non-trivial solutions, the determinant of the coefficient matrix $[A]$ should be zero, resulting in a quadratic algebraic equation for the wave propagating velocity C, which is then solved as

$$C_\pm=V_0\pm C_d \quad (10)$$

$$V_0=\frac{(1-\alpha_0)V_{g0}+\gamma_{pfg}\alpha_0V_{f0}}{(1-\alpha_0)+\gamma_{pfg}\alpha_0} \quad (11)$$

$$C_d=\frac{\sqrt{\alpha_0(1-\alpha_0)\{[(1-\alpha_0)+\gamma_{pfg}\alpha_0]G-\gamma_{pfg}(V_{g0}-V_{f0})^2\}}}{(1-\alpha_0)+\gamma_{pfg}\alpha_0}, \quad (12)$$

where V_0 is defined as the mean velocity of the two-phase flow, and C_d as the amplitude of the dynamic wave velocity relative to the mean motion. From this solution, the K–H instability criterion arrives at once when C_d becomes imaginary as gas velocity increases

$$V_g-V_f\geqslant\sqrt{\frac{G[(1-\alpha_0)+\gamma_{pfg}\alpha_0]}{\gamma_{pfg}}}. \quad (13)$$

Assuming very large density ratio γ_{pfg}, as in the case of air–water flow for instance, we can readily reduce this K–H instability criterion to the form of equation (1). However, the latter results from the second-order equation will illustrate that the viscous wave instability occurs at a much smaller relative gas velocity, especially in the slug or plug transition region.

Since the two coefficient matrixes in equations (9) and (8) are identical, there must exist the following restriction for equation (9) to permit possible solutions

$$\{Z\}^{\mathrm{T}}\{B\} = 0, \tag{14}$$

where $\{Z\}^{\mathrm{T}}$, the left null-space of matrix $[A]$, is defined as

$$\{Z\}^{\mathrm{T}}[A] = 0 \tag{15}$$

$$\{Z\}^{\mathrm{T}} = \left\{-\frac{(V_{g0}-C)}{\alpha_0}, -\frac{\gamma_{pfg}(V_{f0}-C)}{1-\alpha_0}, 1\right\}. \tag{16}$$

After substituting equation (16) into equation (14), we obtain the following ODE with the first-order perturbed variables as functions of time:

$$E\left(\frac{d\alpha_1}{dt}, \frac{dV_{g1}}{dt}, \frac{dV_{f1}}{dt}, \alpha_1, V_{g1}, V_{f1}, \alpha_0, V_{g0}, V_{f0}\right) = 0. \tag{17}$$

In this equation, V_{g1} and V_{f1} can be expressed in terms of α_1 based on the first-order equation

$$V_{g1} = -\frac{V_{g0}-C}{\alpha_0}\alpha_1 \tag{18}$$

$$V_{f1} = \frac{V_{f0}-C}{1-\alpha_0}\alpha_1. \tag{19}$$

Therefore, by replacing V_{g1} and V_{f1} in equation (17) with the solution equations (18) and (19), a first-order ODE containing only α_1 as a dependent variable is obtained in the form of

$$\sigma_1\frac{d\alpha_1}{dt} + \sigma_2\alpha_1^2 + \sigma_3\alpha_1 = 0, \tag{20}$$

where the σs are the functions of the undisturbed variables

$$\sigma_1 = \varphi(\pm C_d)\begin{cases} + \to C_+ \\ - \to C_- \end{cases}, \quad \varphi = 2\frac{\alpha_0\gamma_{pfg} + (1-\alpha_0)}{\alpha_0(1-\alpha_0)} \tag{21}$$

$$\sigma_2 = 3\left\{\gamma_{pfg}\left(\frac{V_{f0}-C}{1-\alpha_0}\right)^2 - \left(\frac{V_{g0}-C}{\alpha_0}\right)^2\right\} \tag{22}$$

$$\sigma_3 = -\zeta(v_w \mp C_d)\begin{cases} - \to C_+ \\ + \to C_- \end{cases}, \quad \zeta = \frac{F'_{V_f}}{(1-\alpha_0)} - \frac{F'_{V_g}}{\alpha_0} \tag{23}$$

$$v_w = \left\{\frac{F'_\alpha - F'_{V_g}(V_{g0}/\alpha_0) + F'_{V_f}[V_{f0}/(1-\alpha_0)]}{F'_{V_f}/(1-\alpha_0) - F'_{V_g}/\alpha_0}\right\} - V_0. \tag{24}$$

In the expression of σ_3, v_w is the so-called 'continuity wave velocity' relative to the mean flow motion defined by Wallis in 1969. All the partial derivatives of F with respect to the dependent variables are evaluated at the equilibrium point. For fixed V_{g0} and α_0, the liquid velocity V_{f0} are solved from the equilibrium equation ($F(V_{g0}, V_{f0}, \alpha_0) = 0$), and the first-order disturbances near the wave front are governed by equation (20). This equation is a standard Riccati equation, which has the following exact analytical solution for a given initial disturbance $\alpha_1(t = 0)$.

$$\alpha_1(t) = \frac{1}{\left[\frac{\sigma_2}{\sigma_3} + \frac{1}{\alpha_1(t=0)}\right]\exp\left(\frac{\sigma_3}{\sigma 1}t\right) - \frac{\sigma_2}{\sigma_3}}. \tag{25}$$

It indicates that evolution of the disturbance α_1 is time dependent. Its behavior, either damped or growing, depends on the coefficients. Consequently, the wave stability boundary can be obtained by solving for the conditions for the initial disturbance to grow without bound as time increases.

STABILITY CRITERIA

In order to compare the results with the small-amplitude wave perturbation theory [1], it is worthwhile to first consider small disturbances. For a small initial disturbance $\alpha_1(t = 0)$, the non-linear term in equation (20) is negligible, and this equation is thus reduced to

$$\frac{d\alpha_1(t)}{dt} = -\frac{\sigma_3}{\sigma_1}\alpha_1(t) = -\frac{1}{\tau}\alpha_1(t). \tag{26}$$

For a given initial disturbance, its solution reads

$$\alpha_1(t) = \alpha_1(t=0)e^{-t/\tau}. \tag{27}$$

Accordingly, a small disturbance will be amplified or damped depending on the sign of the time constant τ. If τ is smaller than zero, i.e. for

$$-\frac{1}{\tau} = -\left(\frac{\sigma_3}{\sigma_1}\right)_{C_i} = -\frac{\zeta(v_w \mp C_d)}{\varphi(\mp C_d)} > 0, \begin{cases} - \to C_+ \\ + \to C_- \end{cases} \tag{28}$$

waves become unstable. Since ζ, φ and C_d are all positive from the definitions, instability occurs when the magnitude of v_w is greater than C_d. For v_w greater than zero, the continuity wave moves faster than the mean flow, and only the forward moving wave with velocity C_+ equal to $V_0 + C_d$ can be unstable. On the other hand, if v_w is smaller than zero, the continuity wave moves slower than the mean flow, and only the backward moving wave with velocity C_- equal to $V_0 - C_d$ can be unstable. This is exactly the same as the conclusion drawn by Wallis in his small amplitude wave perturbation approach. For convenience, these results are termed the linear stability criteria because equation (26) is obtained by neglecting the non-linear term $\sigma_2\alpha_1^2$ in equation (20).

However, the mechanism of the wave instability here is different from the mechanism of wave height growing exponentially with respect to time. Physically, $-\alpha_1$ is the spatial derivative of gas void fraction at the equilibrium point, which is proportional to the slope of the liquid level:

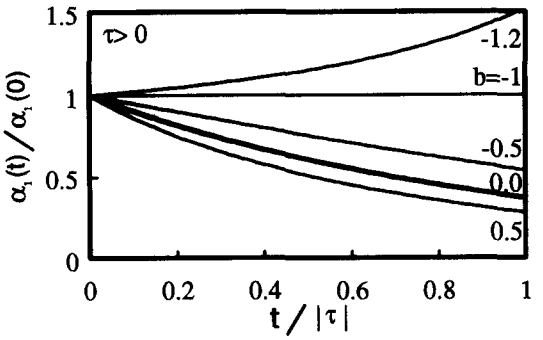

Fig. 2. Transient behavior of $\alpha_1(t)$ with $\tau > 0$ ($b < -1$ unstable).

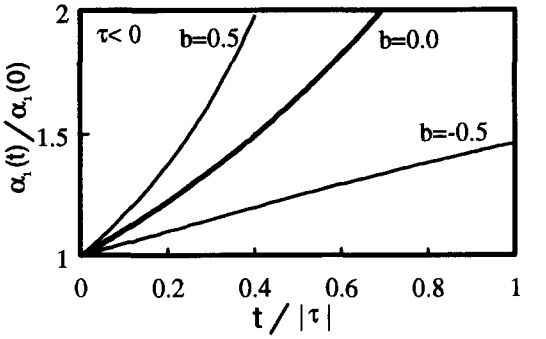

Fig. 3. Transient behavior of $\alpha_1(t)$ with $\tau < 0$ ($b > 0$ unstable).

$$\alpha_1(t) = -\left.\frac{\partial \alpha}{\partial x}\right|_{\alpha=\alpha_0} = \frac{1}{H}\left.\frac{\partial h_f}{\partial x}\right|_{h_f=h_{f0}}. \tag{29}$$

When linear instability occurs, the wave front slope (either positive or negative) becomes steeper and steeper, and eventually breaks. In other words, the linear stability criterion here is the wave-front break-up condition. Since it predicts a critical gas velocity very close to the existing experimental data for slug formation (see next part for detailed comparisons), it is postulated that slug formation is related to the wave front break-up criterion. Following this logic, the weakly non-linear effects can be evaluated with the solution (25). Its non-dimensional form reads

$$\frac{\alpha_1(t)}{\alpha_f(t=0)} = \frac{1}{(b+1)\exp(t/\tau) - b}, \tag{30}$$

where

$$b = \frac{\alpha_1(t=0)\sigma_2}{\sigma_3}.$$

The parameters b and τ determine the evolution of an initial disturbance $\alpha_1(t=0)$. Figure 2 shows the development of an initial disturbance with τ greater than zero, corresponding to the linearly stable condition. With b smaller than minus one, however, α_1 grows to infinity as time increases. Therefore, a wave stable from the linear criteria is predicted to be non-linearly unstable if the initial disturbance satisfies

$$b = \frac{\alpha_1(t=0)\sigma_2}{\sigma_3} < -1. \tag{31}$$

With b approaching zero for either very small initial disturbance or near zero σ_2, α_1 decays in the same way as predicted from the linear solution (the heavy solid line in Fig. 2). On the other hand, for linearly unstable waves ($\tau < 0$), Fig. 3 shows that waves are unstable if b is greater than zero. Namely, any initial wavy disturbance with both front and tail slopes will eventually break.

A rigorous way to find the weakly non-linear wave stability boundary is to examine the conditions for the denominator of equation (30) equal to zero.

$$[b+1]\exp(t_b/\tau) + b = 0, \quad t_b \in (0, +\infty). \tag{32}$$

where t_b denotes the wave breaking time, the time needed for an initial wave slope to grow to infinity, i.e.

$$t_b = \tau \ln\left[\frac{1}{1+1/b}\right], \quad \frac{\alpha_1(t \to t_b)}{\alpha_1(t=0)} \to \infty. \tag{33}$$

For any finite positive solution of t_b, the disturbance is unstable, while τ and b are restricted by the following conditions:

$$\tau = \frac{\sigma_1}{\sigma_3} > 0 \quad \text{and} \quad b = \frac{\sigma_2\alpha_1(t=0)}{\sigma_3} < -1 \tag{34}$$

or

$$\tau = \frac{\sigma_1}{\sigma_3} < 0 \quad \text{and} \quad b = \frac{\sigma_2\alpha_1(t=0)}{\sigma_3} > 0. \tag{35}$$

Thereby, the linearly stable wave may be unstable depending on the initial disturbances. The possible unstable waves that satisfy the linear stability condition are summarized in Table 1. Two types of unstable waves, i.e. roll waves and under-cut waves, can occur under certain flow conditions. An unstable roll wave has a sharpening wave-front slope ($\alpha_1(t) < 0$) and eventually collapses forward, while an unstable under-cut wave has a growing wave-tail slope ($\alpha_1(t) > 0$) and finally breaks backward (Fig. 4). In determining the type of unstable waves, the sign of parameter σ_2 plays an important role. From the definition [equation (22)], σ_2 is related to the non-linear effect of the dynamic pressure difference between the liquid and gas phases. More detailed interpretations will be given later.

When the linear stability condition is satisfied ($\tau > 0$), the wave is unstable if the initial magnitude of α_1 ($t = 0$) is greater than the magnitude of σ_3/σ_2. To demonstrate this criterion, a sinusoidal initial disturbance $\eta = \eta_0 \cos(kCt - kx)$ is taken as an example, where η is measured from the equilibrium interface level and k is the wave number. Because α_1 is proportional to the liquid level slope at the neutral point, the instability criterion can be expressed in the form of

Table 1. Instability conditions and modes

Linear instability	Weak non-linear modification	Wave break mode
$\tau=(\sigma_1/\sigma_3)_+>0$	$\sigma_{2+}>0,\ \alpha_1(0)>\lvert\sigma_3/\sigma_2\rvert_+$, unstable	roll wave
Forward wave is linearly stable	$\sigma_{2+}<0,\ \alpha_1(0)<-\lvert\sigma_3/\sigma_2\rvert_+$, unstable	under-cut wave
$\tau=(\sigma_1/\sigma_3)_-<0$	$\sigma_{2-}>0,\ \alpha_1(0)<-\lvert\sigma_3/\sigma_2\rvert_-$, unstable	under-cut wave
Backward wave is linearly stable	$\sigma_{2-}<0,\ \alpha_1(0)>\lvert\sigma_3/\sigma_2\rvert_-$, unstable	roll wave

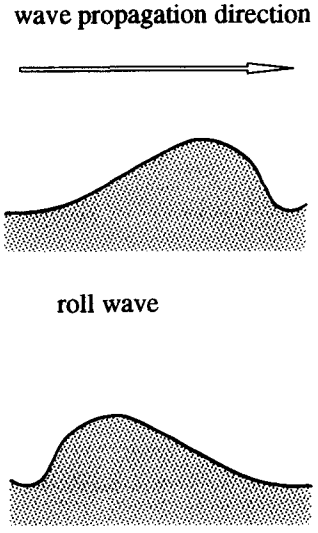

Fig. 4. Schematics of under-cut wave and roll wave.

$$\eta_0 k > H\left|\frac{\sigma_3}{\sigma_2}\right|. \tag{36}$$

With certain equilibrium gas velocity and void fraction, the product of wave height and wave number (or the ratio of wave height to wave length) has a threshold value. Waves will break if $\eta_0 k$ is greater than this limit. A shorter wave has a lower height limit, and a longer wave has a greater height limit. It is quite interesting that a similar criterion for a Stokes wave on an open surface of deep water was obtained by Michell in 1985 [14]. He found that the maximum ratio of wave height to wavelength was 0.142, however, with a completely different approach.

To practically predict the occurrence of wave instability, the shape and the size of the initial disturbance are needed. Nevertheless, as the gas velocity increases, the limit value decreases and finally approaches zero when the continuity wave catches up with the dynamic wave ($\sigma_3=0$). Consequently, waves of any amplitude becomes unstable. Hence, it seems safe to conclude that the linear stability criterion provides a sufficient condition for the formation of unstable waves.

DISCUSSION

It should be emphasized again that the so-called instability here refers to the wave breakage rather than the slug formation. The existing experimental data for the interfacial wave instability in two-phase duct flow are mostly characterized with the onset of slug formation without external excitations. In such circumstances, the disturbances originated from entrance effects or turbulence can be considered very small, with both front and tail slopes. These disturbances will grow and break, sooner or later, due to the relatively small σ_3. As this process continues, the blockage of the flow channel is inevitable, resulting in slug formation. This conclusion agrees with the previous small amplitude perturbation theory. For large disturbances, a smaller gas velocity compared to the prediction of the linear theory can break the waves. If the ratio of the wave height to the wavelength of the newly generated disturbances caused by the wave breakage exceeds the threshold restriction, wave breakage will repeat and eventually induce slug flow. Otherwise, the liquid level will return to the stratified state. Unfortunately, there are no systematic experimental data available for the behavior of the breaking waves, especially for the closed duct two-phase flow. Therefore, it is still uncertain whether the non-linear wave instability would result in slug transition.

Without external disturbances, the linear instability criterion matches the existing experimental data very well. The procedure to find the stability boundary is straightforward. With lumped friction factors at a fixed void fraction, the following critical gas velocity can be obtained explicitly by equating the continuity wave speed v_w to the dynamic wave speed C_d.

$$V_{g0cr}=K\sqrt{\frac{(\rho_f-\rho_g)H\alpha_0 g}{\rho_g}}, \tag{37}$$

where the K factor is

$$K=\sqrt{\frac{(1-\alpha_0)[(1-\alpha_0)+\gamma_{pfg}\alpha_0]}{\alpha_0(1-\alpha_0)\gamma_{pfg}\left(1-\frac{V_{f0}}{V_{g0}}\right)^2+\left(\frac{v_w}{V_{g0}}\right)^2[(1-\alpha_0)+\gamma_{pfg}\alpha_0]^2}}. \tag{38}$$

In the K factor, V_{f0}/V_{g0} and v_w/V_{g0} are independent of V_{g0} [13]. The lumped wall friction factors (f_f and f_g) are assumed to be 0.005 for both the liquid and gas phases in turbulent flow region. The interfacial friction factor f_i is chosen as either equal to or larger than f_g due to the wavy surface analogous to a rough wall. For the air–water flow case, computational results

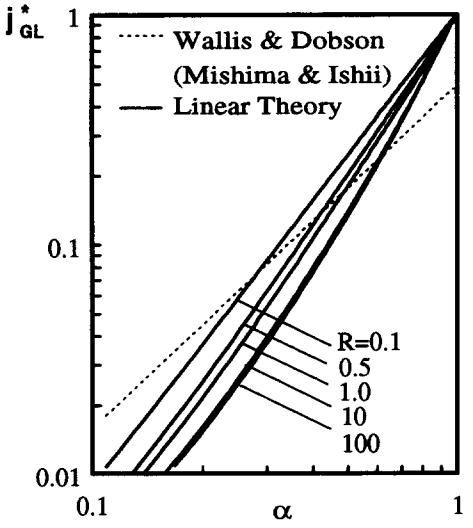

Fig. 5. The onset of slugging in rectangular channel ($R = 0.1 \sim 100$).

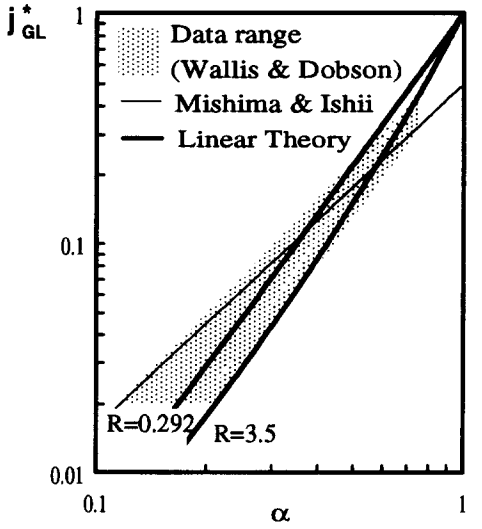

Fig. 6. The onset of slugging in rectangular channel ($R = 0.292 \sim 3.5$).

show that the relative continuity wave velocity v_w is always greater than zero ($0.01 < \alpha_0 < 0.99$) due to the large density difference between water and air. It implies that only the forward wave with velocity $V_0 + C_d$ can be unstable when v_w is greater than C_d. On the other hand, a backward wave with velocity at $V_0 - C_d$ can never be unstable. These phenomena were also observed via the numerical simulation by Barnea and Taitel [12].

In Fig. 5, the linear stability boundaries are plotted with dimensionless relative gas velocity j^*_{GL} against gas void fraction α for different aspect ratio R ($R = W/H$) of a rectangular channel, where j^*_{GL} is defined as

$$j^*_{GL} = (V_{g0cr} - V_{f0})\alpha \sqrt{\frac{\rho_g}{(\rho_f - \rho_g)gH}}. \tag{39}$$

It is concluded that these boundaries depend on the aspect ratio regardless of the channel sizes. A narrow channel with small R needs a higher gas velocity to trigger instability due to the reduction of the fluctuating friction force that is in-phase with the void fraction disturbance. For R greater than 10, the differences are negligible. The dashed line in Fig. 5 represents the following empirical correlation suggested by Wallis and Dobson [2] (also by Mishima and Ishii [7]), which is independent of the channel aspect ratio.

$$V_{g0cr} = 0.5\sqrt{\frac{(\rho_f - \rho_g)gH\alpha}{\rho_g}}. \tag{40}$$

In Fig. 6, a comparison is made between the linear instability criterion and the data of Wallis and Dobson [2] for concurrent air–water flow in a 30.48×8.89 cm rectangular channel. The roof of the channel is adjustable with a fixed water level between 2.54 and 22.86 cm, which corresponds to the aspect ratios ranging from 0.292 to 3.5. With f_i equal to f_g, the linear theory predicts reasonably well the lower stability boundary of the experimental data. Figure 7 shows Kordyban and Ranov's data [6] plotted in j^*_{GL} vs α coordinates. A very interesting empirical correlation for air–waterflow in a 0.7×0.1 m rectangular channel was proposed by Nakamura *et al.* [4]. They found the modifying factor to be 0.3 instead of 0.5. With $f_i/f_g = 1$, Fig. 8 presents an acceptable agreement between linear instability criterion and their experimental data.

Furthermore, according to Table 1, the type of unstable waves can be determined by the sign of σ_2, which represents the non-linear effects. For the case of air–water flow with $f_i/f_g = 1$, Fig. 9 demonstrates that σ_2 is greater than zero when linear or non-near instability occurs for the waves moving forward relative to the mean motion. It indicates that the onset of slug flow regime transition in a horizontal air–water

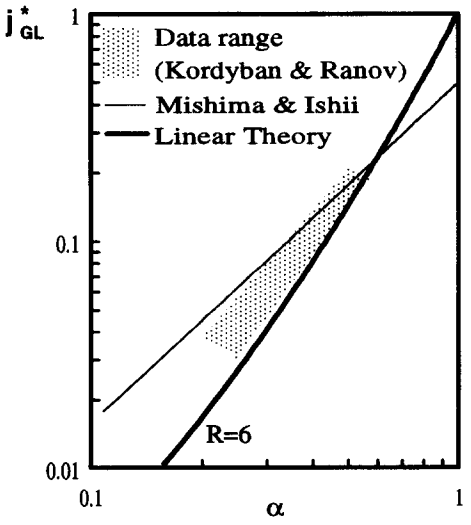

Fig. 7. The onset of slugging in rectangular channel ($R = 6$).

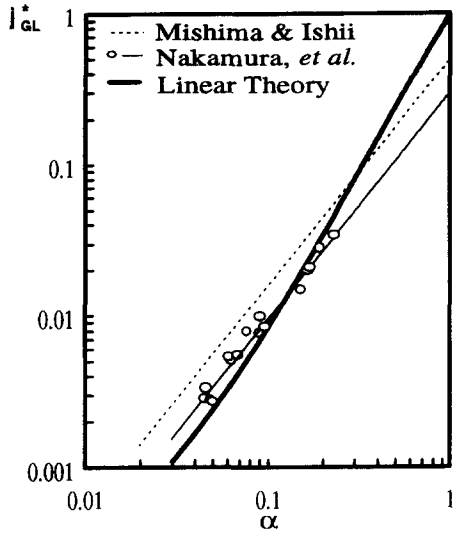

Fig. 8. The onset of slugging in rectangular channel ($R = 7$, $H = 70$ cm, $W = 10$ cm).

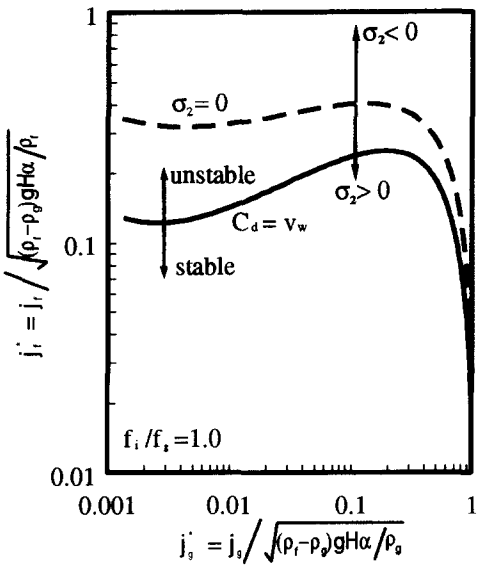

Fig. 9. Types of unstable forward waves with velocity C_+ ($R = 1.0$).

channel flow is caused by roll wave instability. When σ_2 is greater than zero, based on the definition of equation (22) the second-order dynamic pressure fluctuation caused by the first-order velocity disturbance in the liquid phase is higher than that in the gas phase, i.e.

$$\rho_f(V_{f1}\xi)^2 > \rho_g(V_g\xi)^2. \tag{41}$$

At the wave front where the liquid level slope is negative with α_1 less than zero, the pressure difference tends to push the level sharper and sharper when the instability condition is satisfied, resulting in unstable roll waves, while on the front side of a wave, where the liquid level slope is positive, the second order pressure difference has a tendency to suck up the trough of the wave to end the disturbance, resulting in a flat tail level.

CONCLUSION

(1) With the wave front perturbation method, the wave stability boundary is obtained including weak non-linear effects. Its linear instability criterion agrees with the conclusion of small-amplitude wave perturbation technique. Instability happens if the continuity wave velocity is greater than the dynamic wave velocity. For the air–waterflow case, however, only the forward wave can be unstable. Since the initial disturbances are small due to entrance and turbulent effects, linear criterion can be applied to slug or plug formation without significant discrepancy. Fairly good agreement with existing, wide range experimental data is achieved.

(2) In j^*_{GL} vs α coordinates, the linear stability boundaries depend on the channel aspect ratios ($R = W/H$) regardless of the channel sizes. A narrow channel with small R requires larger gas velocity to trigger wave instability, due to the smaller fluctuating friction force that is in-phase with the wave front slope. For R greater than 10, the differences are negligible.

(3) A non-linear wave instability criterion is obtained. Accordingly, linearly stable initial disturbances that are stable based on linear theory can be unstable if their slopes are greater than a threshold value determined by the weak non-linear theory. This threshold value is found to be a function of the mean flow conditions. In order to apply the non-linear stability criterion in practice, information on the initial disturbance is needed. Moreover, linear stability criterion is a sufficient condition for slug formation. Under certain circumstances, such as the existence of large external disturbances, the linear criterion may over predict the critical gas velocity for slug formation.

(4) The types of unstable wave, roll wave or undercut wave, can be predicted with the non-linear parameter σ_2. For the air–water flow case, the onset of wave instability occurs at the front of the waves that move forward relative to the mean motion. This kind of wave is called the unstable roll wave.

(5) Experimental data are needed to examine the wave break-up time or mode for known initial disturbances. A more profound understanding to the slug formation mechanism is expected if the initial disturbance can be controlled or measured in a well designed experimental facility. Furthermore, throughout this study the friction factors are assumed to be constant in order to obtain the insight of the instability mechanism. For an engineering application, it might be too rough to use lumped friction factors.

Acknowledgements—One of us (QW) is grateful for the partial financial support received in the form of a Purdue Research Foundation Fellowship. The authors would like to

express sincere appreciation to Dr V. H. Ransom, Mr I. Babelli and Mr W. H. Leung who made constructive comments on the interpretation of the theoretical results. Finally, the authors wish to extend their thanks to the reviewers for their valuable suggestions.

REFERENCES

1. G. B. Wallis, *One-Dimensional Two-phase Flow*, p. 146. McGraw-Hill, New York (1969).
2. G. B. Wallis and J. E. Dobson, The onset of slugging in horizontal stratified air–water flow. *Int. J. Multiphase Flow* **1,** 173–193 (1973).
3. J. M. Mandhane, G. A. Gregory and K. Aziz, A flow pattern map for gas–liquid flow in horizontal pipes, *Int. J. Multiphase Flow* **1,** 537–553 (1974).
4. N. Nakamura, M. Kondoh, Y. Anoda and Y. Kukita, Horizontal flow regime transition in a large-height long duct, *Proceedings of International Conference on Multiphase Flow*, Vol. 1, pp. 11–14. Tsukuba, Japan (1991).
5. Y. Taitel and A. E. Dukler, A model for predicting flow regime transitions in horizontal and near horizontal gas–liquid flow, *AIChE J.* **22,** 47–55 (1976).
6. E. S. Kordyban and T. Ranov, Mechanism of slug formation in horizontal two-phase flow, *ASME J. Basic Engng* **92,** 857–864 (1970).
7. K. Mishima and M. Ishii, Theoretical prediction of onset of horizontal slug flow, *J. Fluid Engng* **102,** 441–445 (1980).
8. P. Y. Lin and T. J. Hanratty, Prediction of the initiation of slugs with linear stability theory, *Int. J. Multiphase Flow* **12,** 79–98 (1986).
9. H. L. Wu, B. F. M. Pots, J. F. Hollenberg and R. Meerhoff, Flow pattern transitions in two-phase gas/condensate flow at high pressure in an 8-inch horizontal pipe, *Proceedings of 3rd International Conference on Multiphase Flow*, pp. 13–21. The Hague, Netherlands (1987).
10. C. J. Crowley, G. B. Wallis and J. J. Barry, Dimensionless form of a one-dimensional wave model for the stratified flow regime transition, *Int. J. Multiphase Flow* **2,** 369–376 (1993).
11. D. Barnea and Y. Taitel, Structural and interfacial stability of multiple solutions for stratified flow, *Int. J. Multiphase Flow* **6,** 821–830 (1992).
12. D. Barnea and Y. Taitel, Non-linear interfacial instability of separated flow, *Chem. Engng Sci.* **14,** 2341–2349 (1994).
13. G. B. Whitham, *Linear and Non-linear Waves*, p. 130. Wiley, New York (1974).
14. Q. Wu, Transient two-phase flow and application to severe nuclear reactor accident, Preliminary Ph.D. thesis proposal, Department of Nuclear Engineering, Purdue University, West Lafayette, IN (1994).
15. J. H. Mitchell, The highest wave in water, *Phil. Mag.* **5,** 430–442 (1985).